

Opportunistic infection as a cause of transient viremia in  
chronically infected HIV patients under treatment with HAART

Laura E. Jones  
Ecology and Evolutionary Biology  
CORNELL UNIVERSITY  
Ithaca, New York 14853

and

Alan S. Perelson  
Theoretical Biology and Biophysics  
LOS ALAMOS NATIONAL LABORATORY  
Los Alamos, New Mexico 87545

arXiv:q-bio/0411040v1 [q-bio.PE] 19 Nov 2004

## Abstract

When highly active antiretroviral therapy is administered for long periods of time to HIV-1 infected patients, most patients achieve viral loads that are “undetectable” by standard assay (i.e., HIV-1 RNA  $< 50$  copies/ml). Yet despite exhibiting sustained viral loads below the level of detection, a number of these patients experience unexplained episodes of transient viremia or viral “blips”. We propose here that transient activation of the immune system by opportunistic infection may explain these episodes of viremia. Indeed, immune activation by opportunistic infection may spur HIV replication, replenish viral reservoirs and contribute to accelerated disease progression. In order to investigate the effects of concurrent infection on chronically infected HIV patients under treatment with highly active antiretroviral therapy (HAART), we extend a simple dynamic model of the effects of vaccination on HIV infection [Jones and Perelson, *JAIDS* 31:369-377, 2002] to include growing pathogens. We then propose a more realistic model for immune cell expansion in the presence of pathogen, and include this in a set of competing models that allow low baseline viral loads in the presence of drug treatment. Programmed expansion of immune cells upon exposure to antigen is a feature not previously included in HIV models, and one that is especially important to consider when simulating an immune response to opportunistic infection. Using these models we show that viral blips with realistic duration and amplitude can be generated by concurrent infections in HAART treated patients.

## Introduction

Adherence to a regime of highly active antiretroviral therapy (HAART) suppresses the viral loads of most chronically infected HIV patients below the level of detection by standard assay. However, a number of these otherwise well-suppressed patients experience unexplained “viral blips” while on therapy. Di Mascio et al. (2003a) in a study of 123 patients found that the mean blip amplitude was  $158 \pm 132$  HIV RNA copies/ml, with the distribution skewed towards low amplitude blips. In addition, Di Mascio et al. (2003a) suggest that a viral blip is not an isolated event but rather is a transient, intermittent episode of detectable viremia (HIV-1 RNA  $> 50$  copies/ml) with a duration of roughly two to three weeks. They further showed that the amplitude and frequency distribution of these viral transients are consistent with viral load rising sharply, followed by slower, two-phase (double exponential) decay (Di Mascio et al., 2003a). An example of a typical blip is shown in Figure 1 A. The frequency of these episodes appears to be inversely correlated with CD4+ T-cell count at baseline, prior to initiation of drug therapy (Di Mascio et al., 2003a, 2004b). Figure 1 B shows data from the 123 patients in the Di Mascio et al. 2003a study. CD4+ T cell counts at the onset of therapy are plotted against the frequency of blip occurrences per sample, showing a positive correlation between low initial CD4+ counts and blip frequency.

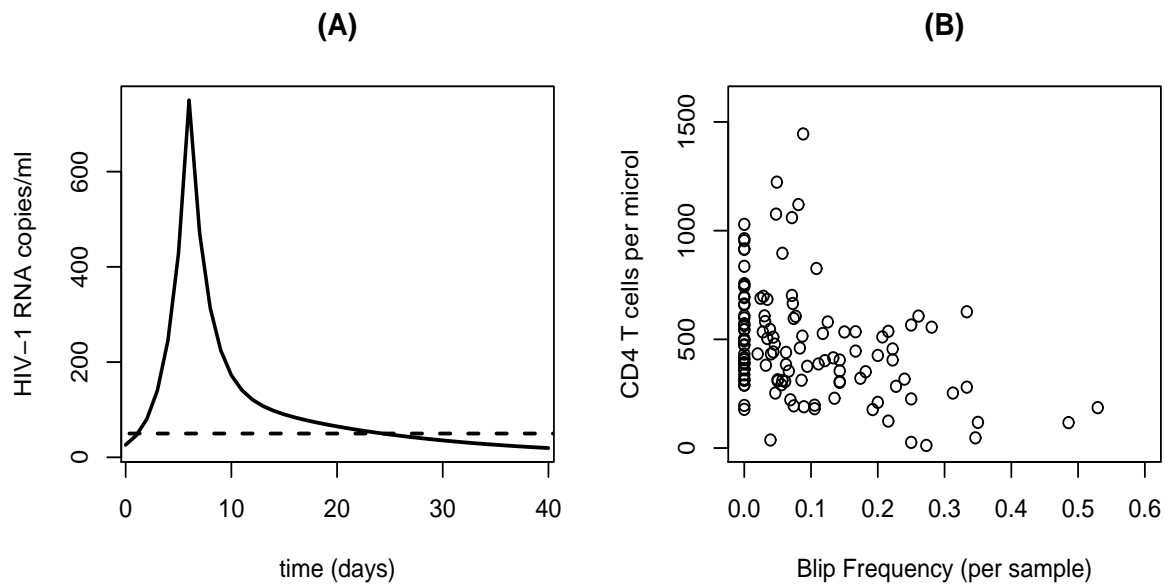


Figure 1: Generalized viral blip shape, and correlation with CD4+ T-cell count at the onset of therapy. A, stylized blip with rapid rise and two-phase exponential decay. Given a mean duration over threshold of 20 to 30 days, the two decay constants assume values of roughly  $0.6$  and  $0.06d^{-1}$  (Di Mascio et al. 2003a), consistent with the mortalities of short lived productively infected cells and longer-lived chronically infected cells. B, CD4+ count at the start of therapy versus viral blip frequency. Both panels after Figure 4 (panels B,C), Di Mascio *et al.* 2003a.

A number of possible causes of blips have been suggested, including but not limited to missed drug doses, activation of latently infected cells and consequent release of virus, release of virus from tissue reservoirs, and a rise in target cell availability due either to vaccination (Jones and Perelson, 2002) or one or more coinfections by opportunistic pathogens, which then increase viral replication. The observation of Di Mascio et al. (2003a) that blip frequency is inversely correlated with baseline CD4+ T cell count suggests that patient specific factors, such as susceptibility to infection, which increases at low CD4 counts, may play a role in blip generation. Prior work on untreated, chronically infected HIV patients documents increases in viral load associated with vaccination (O'Brien et al., 1995; Staprans et al., 1995; Brichacek et al., 1996; Stanley et al., 1996) and with opportunistic infection (e.g., Donovan et al., 1996). McLean and Nowak (1992) proposed some of the first models of enhanced HIV replication due to immune stimulation via opportunistic infection, and showed how the positive feedback between enhanced HIV replication and incomplete immune control of pathogens due to HIV-immunosuppression leads finally to immune failure and full-blown AIDS.

This paper examines the hypothesis that viral blips result from random encounters with replicating antigens - or transient opportunistic infections in HIV positive patients. We begin with a simple model for coinfection, explore its biological shortcomings, and develop a series of incrementally more complex models. To minimize the introduction of new parameters while accurately simulating the dynamics of transient viremia, we add missing biology at each step and then test each incremental model to see where it falls short and where it is sufficient. In the process, we introduce biologically realistic mechanisms for programmed immune cell proliferation, and include features which allow robust low viral loads under drug treatment.

## A simple model for coinfection

We begin with the following simple model for coinfection in the presence of HIV infection, which is a generalization of the HIV infection model developed by Perelson et al. (1996, 1997) and reviewed by Perelson (2002).

$$\frac{dA}{dt} = r_0 A \left(1 - \frac{A}{A_{max}}\right) - \gamma AT \quad (1a)$$

$$\frac{dT}{dt} = \lambda + a \left(\frac{A}{A + K}\right) T - d_T T - (1 - \epsilon) k VT \quad (1b)$$

$$\frac{dT^*}{dt} = (1 - \alpha)(1 - \epsilon) k VT - \delta T^* \quad (1c)$$

$$\frac{dC}{dt} = \alpha(1 - \epsilon) k VT - \mu C \quad (1d)$$

$$\frac{dV}{dt} = N_T \delta T^* + N_c \mu C - cV \quad (1e)$$

Here the antigen,  $A$ , is a growing pathogen,  $T$  are uninfected CD4+ T cells,  $T^*$  are cells productively infected with HIV,  $C$  are cells chronically infected with HIV, and  $V$  represents HIV-1 (RNA copies/ml). Pathogen  $A$  undergoes density-dependent growth described by a logistic law with maximum growth rate  $r_0$  and carrying capacity  $A_{max}$ . As in earlier work by Jones and Perelson (2002), we assume that the antigen is cleared in a T cell-dependent manner with rate constant  $\gamma$ . We further assume that uninfected T cells,  $T$ , are generated at rate  $\lambda$ , die at rate  $d_T$ , and are infected by virus with rate constant  $k$ . Assuming reverse transcriptase (RT) inhibitors are administered, the infectiousness of the virus  $k$  is reduced by  $(1 - \epsilon)$ , where  $\epsilon$  is the efficacy of the RT inhibitors and  $0 \leq \epsilon \leq 1$ .

In this simple model we assume T cells are activated into proliferation at a maximum rate  $a$  in the presence of pathogen, and that the proliferation rate depends on the pathogen concentration with a half-saturation constant  $K$ . HIV infection of T cells results in productively infected cells  $T^*$ , which die at a rate  $\delta$ , and chronically infected cells  $C$ , with mortality  $\mu < \delta$ . A fraction of infection events  $\alpha \ll 1$  results in chronic infection. Chronically infected cells live much longer, producing virus more slowly than productively infected cells. The inclusion of the chronically infected pool is motivated by the suggested two-phase decay of a viral transient (Di Mascio et al., 2003a).

Finally, virus is produced by productively and chronically infected cells at rates  $N_T \delta$  and  $N_C \mu$ , respectively, where  $N_T$  and  $N_C$  are average burst sizes for productively and chronically infected cells. Virus is cleared at a constant rate  $c$  per virion.

Based on previous work we take as a typical set of parameter values  $\lambda = 1 \times 10^4 \text{ ml}^{-1}$ ,  $k = 8 \times 10^{-7} \text{ ml/d}$ ,  $\alpha = 0.195$ ,  $N_T = 100$  and  $N_C = 4.11$  (Callaway and Perelson, 2002);  $d = 0.01 \text{ d}^{-1}$  (Mohri et al., 1998);  $\delta = 0.70 \text{ d}^{-1}$  and  $\mu = 0.07 \text{ d}^{-1}$  (Perelson et al., 1997); and  $c = 23 \text{ d}^{-1}$  (Ramratnam et al., 1999). The antigen or pathogen clearance rate constant  $\gamma$  is a ‘‘fitted’’ parameter, which we set to  $1 \times 10^{-3} \text{ ml d}^{-1}$ . In a prior study of the effects on viral load of vaccination (with a non-replicating antigen), this fitted value varied widely from patient to patient with values roughly  $1 \times 10^{-5}$  to  $1 \times 10^{-8} \text{ ml d}^{-1}$ , reflecting differences in patient immune response (Jones and Perelson, 2002). We assumed a higher clearance rate in

this study since immune activation by a proliferating pathogen should be much greater than activation due to a small dose of non-replicating antigen. Note that where these parameters are used elsewhere in this paper, they retain the above values unless otherwise noted.

In the absence of pathogen, and assuming chronic HIV infection, the viral load stabilizes at the following equilibrium state:

$$\bar{V} = \frac{\lambda}{c}[(1 - \alpha)N_T + \alpha N_c] - \frac{d}{(1 - \epsilon)k}, \quad (2)$$

implying an inverse relationship between steady state viral load and drug efficacy  $\epsilon$ .

This model without the inclusion of drug therapy, i.e.  $\epsilon = 0$ , and with a non-growing pathogen, i.e.,  $r_0 = 0$ , worked surprisingly well for modeling HIV dynamics in chronically infected, untreated patients following vaccination with a common recall antigen (Jones and Perelson, 2002).

However, this model does not generate realistic blips when a growing pathogen is substituted for a vaccine. There are several reasons for this: even in untreated patients, according to our model, T-cells respond very rapidly, eliminating the pathogen before it has time to grow (Figure ?? A), so there is only a relatively small immune response to the presence of the pathogen, and little change in viral load (Figure ?? B). The system remains relatively unaffected by increases in pathogen growth rate until  $r_0$  reaches a critical point where the model immune system cannot completely eliminate the pathogen, and then there are predator-prey cycles. [Note that inclusion of a logistic growth term means that the pathogen can reach a carrying capacity,  $A_{max}$ , but will not experience runaway growth.] With the addition of drug therapy (Figure ?? C) of efficacy  $\epsilon = 0.6461275$  (see Appendix), baseline viral load is suppressed to 25 RNA copies ( $\text{ml}^{-1}$ ) and opportunistic infection results in a small, slow rise and fall in viral load, rather than a burst of viremia. If baseline viral load is suppressed further, then there is no appreciable change in viral load.

## Building a new model

While different parameters could be explored, we believe that there is a need to generate more biologically realistic models. First, the majority of patients with viral loads below 50 copies/ml who have been examined with more sensitive assays have viral loads that are still detectable, i.e. been 1 and 50 copies/ml (Dornadula et al.,1999, Di Mascio, 2003b). This suggests that appropriate models must exhibit robust low viral steady states for patients on therapy. By contrast, the model given by eqs. (1) requires drug efficacy  $\epsilon$  precisely tuned to many decimal places in order to yield a low, yet not vanishingly small, viral steady state (Callaway and Perelson, 2002). Second, recent immunological data suggest

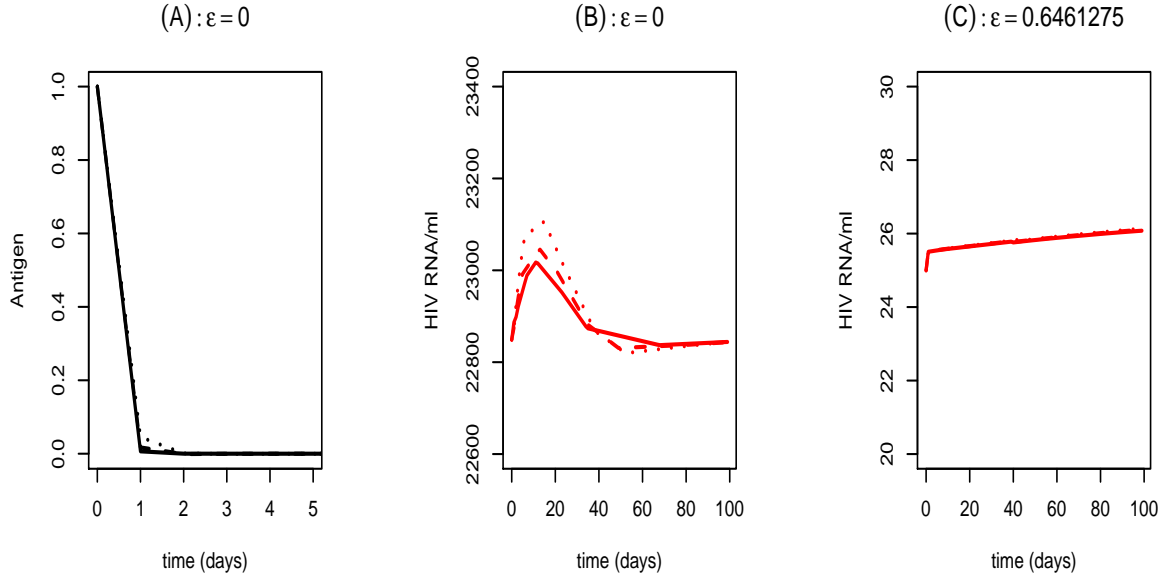


Figure 2: Simulations of a simple coinfection model (1) for pathogen growth rates  $r_0 = 1, 2, 3, 4$   $\text{day}^{-1}$  (solid, dashed, dotted line in each panel) given no drug treatment (panels A, B) and treatment with a drug of efficacy  $\epsilon = 0.6451275$  (panel C). A, Antigen growth assuming  $\epsilon = 0$  and  $A_0 = 1$ ; B Viral load (HIV-1 RNA/ml) assuming  $\epsilon = 0$ ; C, Viral load (HIV-1 RNA/ml) assuming  $\epsilon = 0.6461275$ . Baseline VL is 25 RNA copies/ml.

T-cell proliferation stimulated by a pathogen involves a cascade of divisions, all triggered by a brief exposure to antigen. Models should thus account for this type of “programmed” response. Lastly, immune response to a pathogen involves generation of effector cells that are responsible for clearing the pathogen. For many viral infections, CD8+ T cells are critical for containing and clearing the infection (Wong and Palmer, 2003). This is well documented in lymphocytic choriomeningitis virus (LCMV) infection, where a strong antigen-specific CD8+ T cell response is induced, leading to rapid elimination of the virus (Murali-Krishna et al., 1998a,b).

## T-cell proliferation under antigenic stimulation

Upon exposure to antigen, naive CD8+ T cells undergo a burst of proliferation, entering a programmed cascade of divisions that culminate in the production of mature, activated effector cells (Kaech and Ahmed, 2001). This is followed by a programmed contraction in which most of the effector cells are subject to apoptosis, leaving a small, stable memory population (Badovinac et al, 2002). Revy et al. (2001) proposed a system of ordinary differential equations to analyze and describe T-cell proliferation. We adapt their model to incorporate activation by a growing pathogen,  $A$ , which is finally cleared by CD8+ effector cells,  $E$ .

$$\text{Antigen } \frac{dA}{dt} = r_0 A \left(1 - \frac{A}{A_{max}}\right) - \gamma A E \quad (3a)$$

$$\frac{dN_0}{dt} = -(p_0(A) + d_0) N_0 \quad (3b)$$

$$\text{CD8 Response } \frac{dN_1}{dt} = 2p_0(A) N_0 - (p + d) N_1 \quad (3c)$$

$$\frac{dN_i}{dt} = \begin{cases} 2p N_{i-1} - (p + d) N_i, & i = 2, 3, 4. \\ 2p N_{i-1} - (p + d_E) N_i, & i = 5, \dots, k - 1. \end{cases} \quad (3d)$$

$$\frac{dN_k}{dt} = 2p N_{k-1} - d_E N_k \quad (3e)$$

Here again  $A$  is an opportunistic pathogen,  $r_0$  is the pathogen growth rate, and  $\gamma$  is the clearance rate constant for the pathogen.  $p_0$  and  $p$  are constant proliferation rates,  $N_0$  is the initial, naive cell pool, and the  $N_i$  are proliferative phases, or “division classes”: for each  $i$ , the number of cells that have completed  $i$  divisions, and  $E$  are mature, pathogen-specific “effector” cells. As the CD8+ T cells proliferate they also differentiate into effectors,  $E$ . Here we assume cells become effectors after 4 divisions and stop proliferating after 8 division;  $E = \sum_{i=4}^8 N_i$ . Alternatively, one could assume a fraction of cells,  $\beta_i$ , become effectors after  $i$  divisions, i.e.,  $E = \sum_{i=1}^8 \beta_i N_i$ , or leave the maximum number of divisions as an adjustable parameter. Proliferative, non-effector phases (division classes  $N_0, N_1, \dots, N_3$ ) undergo mortality at a rate  $d \ll d_E$ , the death rate for activated effector cells.

Experiments suggest that when quiescent cells are stimulated into proliferation, the initial cellular division takes longer than subsequent divisions (Gett and Hodgkin, 2000), and that the time to first division depends on features of the antigen stimulation. For example, using anti-CD3 antibodies rather than antigen to stimulate CD8+ T cells, Deenick et al. (2003) found that decreasing the anti-CD3 concentration lengthened the time to first division. We thus assume the rate of the first CD8+ T cell division depends on antigen according to a Type-III functional response,

$$p_0(A) = p_0 \frac{A^n}{(A^n + K_8^n)} \quad (4)$$

where  $K_8$  represents the critical antigen level required to stimulate a CD8+ response [Table I]. Thus when  $A$  is low, i.e.,  $A \ll K_8$ , growth is slow, whereas when  $A$  attains values greater than  $K_8$  rapid growth ensues, saturating at rate  $p_0$ . Here  $n$  is a parameter frequently called the Hill coefficient and it determines the steepness of the response when  $A$  is near the “threshold”  $K_8$ .

While the initial division may be relatively slow, subsequent divisions occur more rapidly, without an initial delay, as cells are already activated. These divisions occur even if antigen



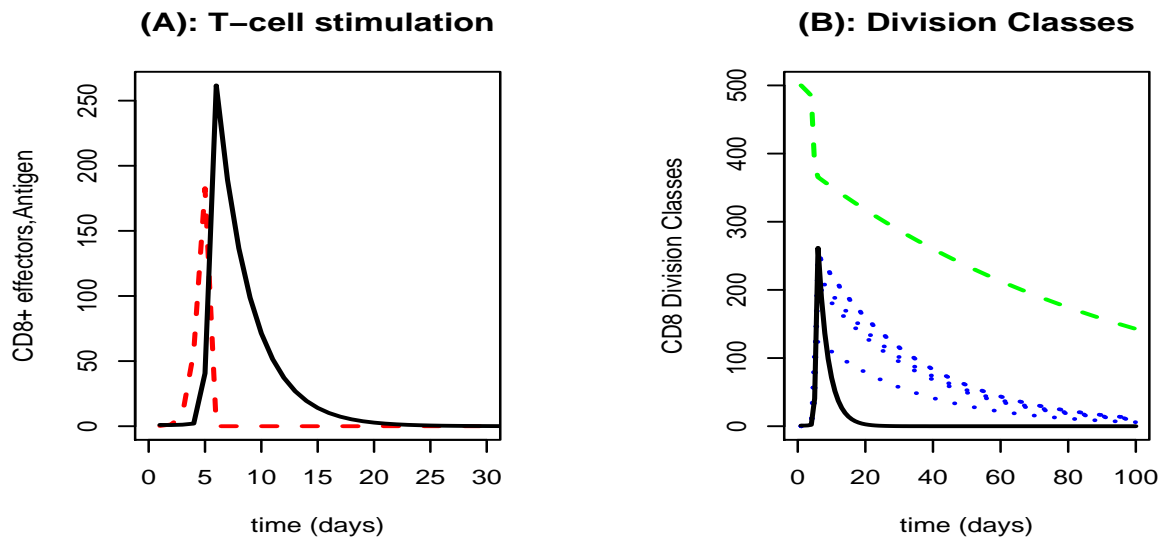


Figure 3: Simulated results for CD8+ T-cell proliferation stimulated by a growing antigen. A, antigen ( $A_0 = 1$ ), shown in dashed red line; total CD8+ effector cells (solid black line). B, cell counts for the various division classes (dotted blue); total effectors ( $\sum_{i=4}^8 N_i$ ) (solid black line), and naive cells (dashed green line). Since the process of proliferation is a cascade involving both growth and mortality and we assume growth is more rapid than mortality each successive division class is slightly larger than the preceding class. The effector population (black line) is subject to higher mortality than the less differentiated preceding classes.

is removed (Badovinac et al., 2002). We therefore assume subsequent divisions occur at a constant rate,  $p > p_0$  (Table 1).

In the model we do not explicitly account for precursor cells that fail to divide, although in the experiments by Gett and Hodgkin (2002) such cells are present.

Based on CD8+ T-cell response estimates for LCMV in mice (De Boer et al., 2001), we set  $p = 2.92 \text{ d}^{-1}$ , and chose the initial activation/first division rate  $p_0 = 1 \text{ d}^{-1}$ . The initial quiescent cell pool is small,  $N_0 = 500 \text{ cells/ml}$ : it is estimated that one in  $10^5$  T cells is specific for any given epitope, and assuming that a healthy human being has roughly  $10^{11}$  CD8+ T cells, we expect about  $10^6$  antigen-specific cells. Most naive cells are in lymphoid tissue, which in a 70 kg man weighs about 700 grams. Thus, with some cells circulating in the blood and others not naive, a density of about 500 cells/ml in lymphoid tissue, where most proliferation occurs, seems appropriate.

Figure 3 shows results from simulation of equations (3). In this simulation, we assume eight division classes,  $N_i$ ,  $i = 1, \dots, 8$ , plus naive cells,  $N_0$ , with effector cells,  $E$ , corresponding to the sum of the last four division classes. In panel A, the growing antigen (dashed red line), and CD8+ effectors (solid black line) are shown. Panel B shows the CD8+ T cells in the various division classes and the mature effector cells. Note that effector pool grows and is

depleted within the first 20 days, while the proliferating cells that have not differentiated into effectors are longer lived.

### Density-dependent infected cell death

In the simple coinfection model (1), infected cells are assumed to have constant mortality:  $\delta$  for productively infected cells,  $T^*$ , and  $\mu$  for chronically infected cells,  $C^*$ , respectively. In this model under very effective drug therapy the steady state viral load becomes vanishingly small. However, if the death of infected cells is made density dependent, as one might expect when infected cell death is immune-system mediated and immune response is a function of the number of infected cells present, then low steady state viral loads are possible (Callaway and Perelson, 2002).

Here we assume that the magnitude of the immune response against HIV-infected cells, and thus their death-rate, is an increasing function of the infected cell density (Callaway and Perelson, 2002). Holte et al. (2001), fitting data on viral decays in HIV treated children, suggested that this can be modeled by a power law, that is, by replacing the constant  $\delta$  with a function  $\delta^*(T^*)$  that depends on the total number of infected cells raised to a power  $\omega$

$$\delta^*(T_{total}^*) = \delta'(T_{total}^*)^\omega \tag{5}$$

and the constant  $\mu$  with

$$\mu^*(T_{total}^*) = \mu'(T_{total}^*)^\omega$$

where  $\omega < 1$  and  $T_{total}^* = T^* + C$  is the total number of HIV-infected cells, which represents the stimulus for a cell-mediated response to HIV-infection.

In the following series of models employing density-dependent infected cell death, we explore various scenarios for CD8+ mediated immune responses to an opportunistic infection.

### Simplest case: An HIV infection model with programmed proliferation of CD8+ T cells

We now combine the basic HIV infection and treatment model with CD8+ T cell response to pathogen in the form of the programmed proliferation model described above. Since the effector cells are pathogen specific, not HIV specific, the dynamics of the CD8+ T cell population remains decoupled from the HIV infection model, except through their indirect

effect on the pathogen. To the model for programmed proliferation of effector cells under antigenic stimulation (equations 3) we add the following model for HIV infection with density dependent mortality of infected cells:

$$\frac{dT}{dt} = \lambda + f(A)T - (1 - \epsilon)kVT - d_T T \quad (6a)$$

$$\frac{dT^*}{dt} = (1 - \epsilon)(1 - \alpha)kVT - (\delta^*(T_{total}^*))T^* \quad (6b)$$

$$\frac{dC}{dt} = \alpha(1 - \epsilon)kVT - \mu^*(T_{total}^*)C \quad (6c)$$

$$\frac{dV}{dt} = q_1 T^* + q_2 C - cV \quad (6d)$$

Target cells,  $T$ , are activated by antigen following a type-II functional response, as in the basic model

$$f(A) = a \frac{A}{A + K_4} \quad (7)$$

and are susceptible to infection by HIV at a rate  $k$ . We do not separate out antigen-specific CD4+ cells; instead we let the activation parameter  $a$  incorporate the fact that only a fraction of CD4+ cells in that pool may be activated by antigen.

Because the model includes density-dependent cell death, we decouple viral production rates from cell death rates, and assume virus is produced at constant rates  $q_1 = N_T \delta = 70 \text{ d}^{-1}$  and  $q_2 = 0.28 \text{ d}^{-1}$ , from short-lived and chronically-infected cells, respectively. Rate constants and parameters describing the proliferating CD8+ pool remain as above. A listing of additional fixed parameter values can be found in Table 1.

Figure 4 shows that this model can generate transient viral load increases. Panel A shows that the pathogen initially grows and then is cleared (dashed line) as the effector cells (solid line) increase. Pathogen growth and clearance rates are variable, but for this example we assume  $r_0 = 2 \text{ d}^{-1}$ , and clearance rate constant  $\gamma = 1 \times 10^{-3}$ . The effect of this pathogen growth is to stimulate increased infection and viral production (Fig. 4B). As drug treatment is assumed, CD4+ levels can be quite high, leading to an unrealistic number of activated target cells, and excessively large increases in viral load. Thus while the model does indeed produce viral transients, there is a tradeoff between the height and the width of the resulting “blip”. That is, one can obtain an appropriately narrow spike in viremia but it is unrealistically large, or one can obtain a blip of appropriate amplitude (i.e., 100-1000 copies/ml, cf. Di Mascio et al. 2003a) but of unreasonable duration (upwards of 100 days).

In our simulations, parameters associated with steady-state baseline viral load are fixed as discussed above and in the Appendix, and parameters associated with pathogen growth and CD4+ activation are considered variable. Results from sensitivity testing of the model

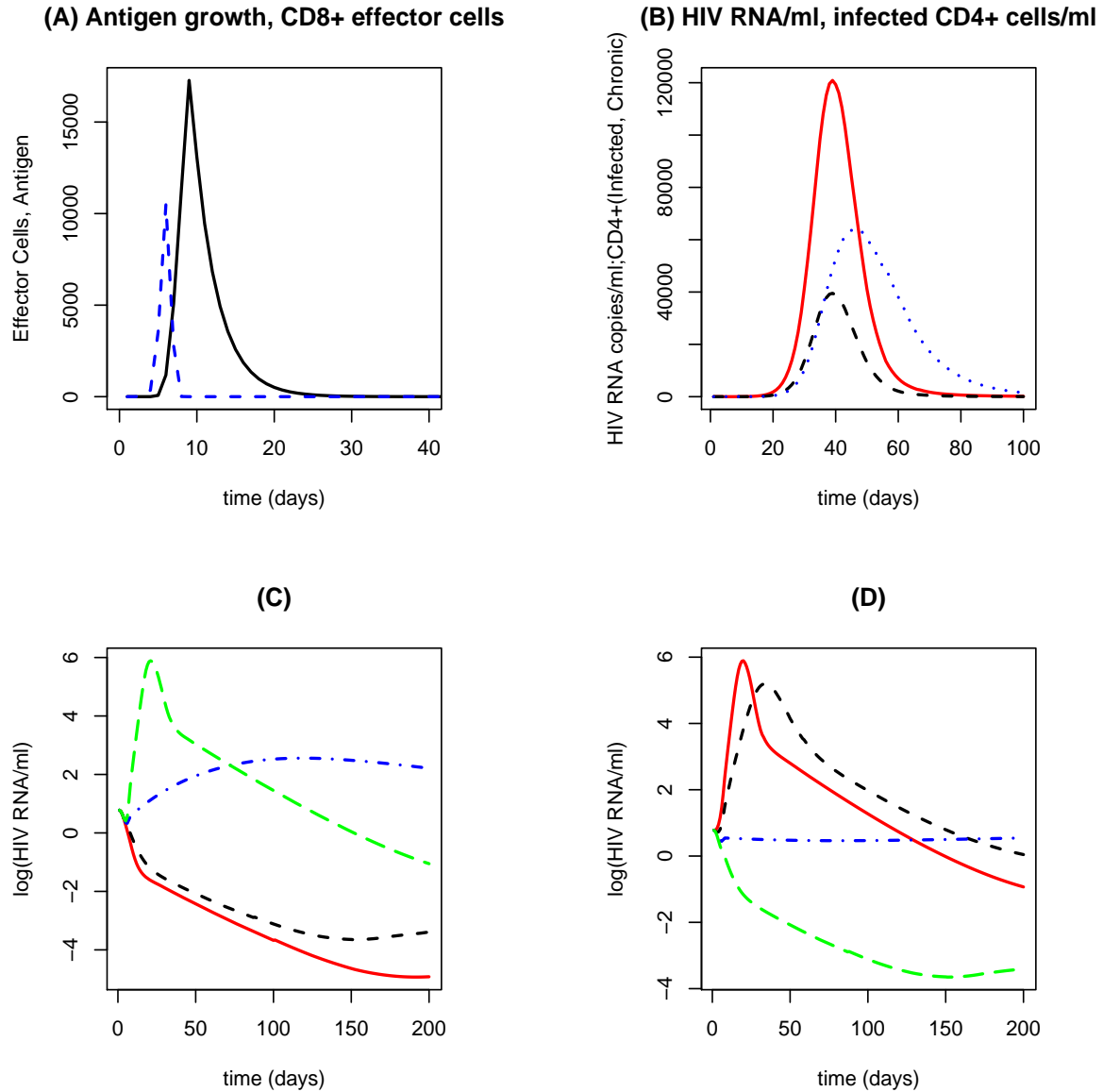


Figure 4: Simulations and sensitivity testing of equations (6,4,7). A, Antigen growth (dashed line) and CD8+ effector cells (solid line); B, Viral load (RNA copies/ml, in solid line), productively infected cells ( $ml^{-1}$ , dashed line), and chronically infected cells ( $ml^{-1}$ , dotted line); C, Viral load (copies/ml) from sensitivity testing of CD4+ T cell activation parameter  $a$ , as  $a$  assumes the values  $a = 0.25, 0.50, 0.75, 1$  (solid, dashed, dash-dotted and long-dashed line, respectively).  $r_0 = 2$  in this example. D, Viral load (copies/ml) from sensitivity testing of pathogen growth  $K_4$ , as  $K_4$  assumes the values  $K_4 = 1, 10^1, 10^2, 10^3$   $d^{-1}$  (solid, dashed, dash-dotted and long-dashed line, respectively). Note that activation parameter  $a$  is held at 0.5 when not varied.

(varying of parameters associated with activation of target cells in response to pathogen growth and especially the growth of the pathogen itself) are shown in Figures 4C and D. The model is very sensitive to changes in the CD4+ T cell activation rate  $a$ : between the values  $a = 0.25 \text{ d}^{-1}$  and  $a = 0.75 \text{ d}^{-1}$ , the model goes from producing no viral transient to producing an unreasonably large viral transient (Figure 4C). Variation in the half-saturation of pathogen load required for CD4+ stimulation,  $K_4$ , shows the opposite trend: as the value of  $K_4$  and thus the pathogen load required for CD4+ stimulation increases, resulting viral transients go from being excessively large (Figure 4D, red line), to non-existent.

Variation in  $r_0$  shows that beyond a threshold value there is relatively small variation in blip peak amplitude with substantial, though biologically reasonable, variation in pathogen growth rate (results not shown).

Interestingly, this model exhibits a delay between the peak in opportunistic infection and the peak in viremia (Figure 4B). The delay appears to be related to the time it takes for the T cell pool to increase and generate a rise in the numbers of infected cells,  $T^*$  and  $C$ , which then in turn generate more virus. As one sees (in Figure 4C), increasing the CD4+ T cell activation rate causes the peak in viremia to occur earlier. Whether these delays are realistic is unknown, but because antigen-specific CD4+ cells and “non-specific” CD4+ cells are all in the same pool and the pool has the relatively low mortality appropriate for “resting” cells, the T cell response may not be realistically modeled.

### **Including separate antigen-specific and non-specific target pools**

In the prior model, the entire CD4+ pool was activated by antigen, resulting in an overly large target population and correspondingly large viral transients. To make the model more realistic, we now divide the target (CD4+) cells into non-specific and antigen-specific pools,  $T$  and  $T_A$ , respectively, where only the antigen-specific CD4+ T cells are activated by antigen. We couple the model for antigen-induced response of CD8 effectors (3) with the following model for HIV infection of antigen-specific and non-specific CD4 cells:

$$\text{Antigen-specific CD4} \quad \frac{dT_A}{dt} = \nu\lambda + f(A)T_A - (1 - \epsilon)k_A VT_A - d_{T_A} T_A \quad (8a)$$

$$\frac{dT_A^*}{dt} = (1 - \epsilon)k_A VT_A - (\delta^*(\omega))T_A^* \quad (8b)$$

$$(8c)$$

$$\text{non-specific CD4} \quad \frac{dT}{dt} = (1 - \nu)\lambda - (1 - \epsilon)kVT - d_T T \quad (8d)$$

$$\frac{dT^*}{dt} = (1 - \epsilon)(1 - \alpha)kVT - (\delta^*(\omega))T^* \quad (8e)$$

$$\frac{dC}{dt} = \alpha(1 - \epsilon)kVT - \mu^*(\omega)C \quad (8f)$$

$$\frac{dV}{dt} = q_1 T^* + q_2 C + q_3 T_A^* - cV \quad (8g)$$

where  $E = \sum_{i=4}^8 N_i$ , and  $p_0(A)$  is defined in (4) and  $f(A)$  defined in (7).

Antigen-specific CD4+ T cells,  $T_A$ , are assumed to be small fraction  $\nu$  of the CD4+ pool  $T$  (see Table 1), and are activated by antigen following a type-II functional response, as in (7). The value of  $\nu$  is poorly defined, and may vary widely from roughly  $10^{-5}$  to  $10^{-2}$  (percent activated 0.001% to 0.1%, respectively). Response to a particular epitope generally occurs at a frequency of about  $10^{-5}$  (0.001%), but a pathogen has many epitopes, thus as many as 10 to 20 responses might occur for a single pathogen, yielding a frequency of  $10^{-4}$  (0.01%). However, if one considers levels of activation in HIV-infected versus healthy people, one finds that in HIV-infected people, roughly 6.5% of CD4+ T cells are activated, depending on total CD4+ count, versus about 1% in healthy individuals. This level of activation might reflect responses to a number of pathogens, or in the case of immuno-compromised HIV patients, may be a homeostatic response to low CD4+ T cell counts. Based on these considerations, we choose a frequency  $\nu = 0.01$ , corresponding to an activated fraction of about 1%. (Note that we could easily choose a slightly higher or lower fraction and obtain similar results by adjusting the activation parameter,  $a$  (7)).

Once activated, target cells are subject to infection by HIV at an increased rate  $k_A$ . The subsequent increase in viral load results in increased infection of the non-specific pool,  $T$ . Both infected antigen-specific  $T_A^*$  and infected non-specific cells  $T^*$  are cleared in a density dependent fashion. Rate constants and parameters for the proliferating CD8+ pool remain as above. Analysis of SIV infection of resting and infected CD4+ T-cells suggests that activated, infected CD4+ cells produce on average twelve times more virus than non-activated infected cells (Zhang et al., 2004). We thus set  $q_3 \doteq 12q_1$  in equations (8).

Using density-dependent infected cell death, the model can produce realistically low baseline viral loads under treatment. For this example the baseline viral load is about 3 RNA copies per ml. Opportunistic infection results in detectable viral transients (Figure 5A), with the stimulus for induced replication arising from the (small) antigen-specific CD4+ T cell pool,

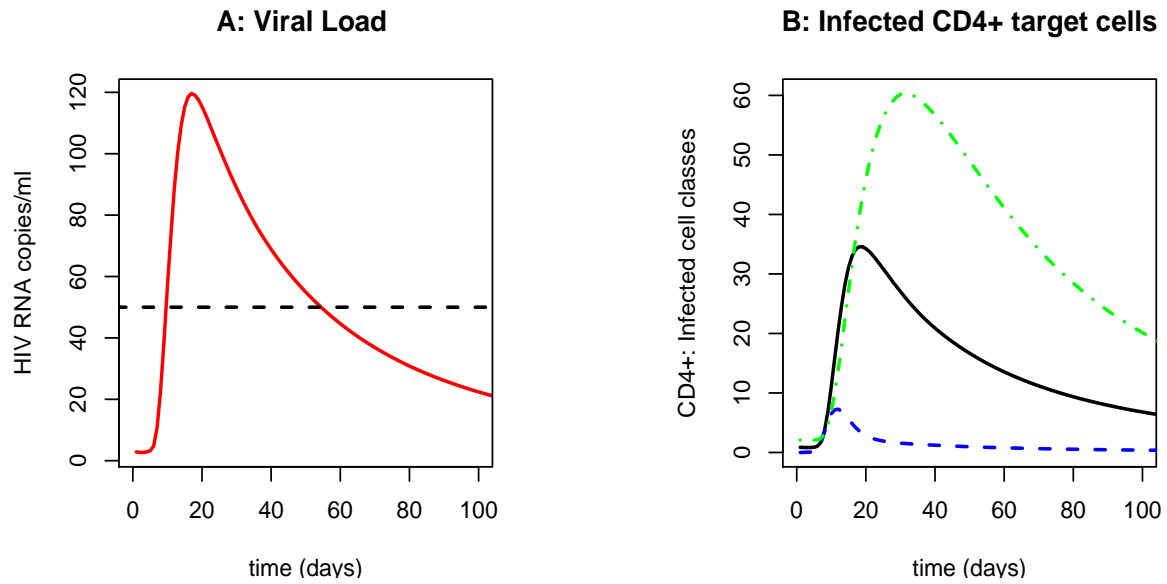


Figure 5: Simulation of equations (8) for a patient assumed to be in steady state with  $\bar{V} \doteq 3$  copies/ml. At  $t = 0$  a pathogen (initial value  $A_0 = 1$ ), growing at rate  $r_0 = 2.0 \text{ days}^{-1}$ , is encountered and eliminated by an immune response with rate constant  $\gamma = 1 \times 10^{-3}$ . Here  $\nu = 0.01$ ,  $\epsilon = 0.62$ ,  $a = 1.2$ ,  $K_8 = 1000$ ,  $K_4 = 100$ . A, Viral load (copies/ml). Dashed line shows limit of assay detection at 50 (copies/ml). B, Non antigen-specific productively infected (solid line) and chronically infected (dashed-dotted line) CD4+ cells, as well as antigen-specific infected CD4+ cells (dashed line), increased by a factor of 10 to better show dynamics.

but most of the increase in viral load coming from infection of antigen non-specific T cells (Figure 5B). The resulting transients have a sharp rise-time and a slow decay, consistent with observation (Di Mascio et al., 2003a). However, blip duration is generally too long, upwards of 30 to 90 days, respectively, for transients of reasonable amplitude (100-1000 RNA copies per ml).

In addition, the model is very sensitive to changes in the parameters  $a$  and  $K_8$ , with less extreme variability in viral load resulting from variation of the pathogen growth parameter  $r_0$  and the half-saturation parameter  $K_4$  (Figure 6). Small variation in the CD4+ cell activation parameter  $a$  alone results in a spectrum of behavior from no detectable viremia to excessively large bursts in viral replication (Figure 6 A). In addition, though in general infectivity  $k$  is poorly constrained, infectivity for activated antigen specific cells  $k_A$  must be set at levels fifteen times higher than that of quiescent cells to produce detectable viremia, and this may not be realistic.

#### *Effects of parameter variation*

- Varying the CD4+ activation parameter,  $a$ , results in large changes in peak viremia over a relatively small range of parameter values, as in Figure 6A. Note that blip durations (i.e., decay times) are too long in all of these examples, and only begin to become shorter with increased values of  $a$  (i.e., greater proportions of the transient arising from infection of activated, antigen-specific cells).
- Increasing  $r_0$  results in more aggressive pathogen growth and swifter CD8+ immune response. For lower values of  $r_0$ , the CD8+ response is delayed, and  $f(A)$  (7) remains elevated longer. A smaller  $r_0$  thus results in a larger amplitude viral transient, with  $r_0 = 1 \text{ days}^{-1}$  resulting in the largest blip, and successively larger values of  $r_0$  resulting in smaller blip sizes (Figure 6B).
- Increasing the half-saturation constant for CD8+ proliferation,  $K_8$  in (4) has a *positive* effect on the sizes of the resulting viral transients, as this allows greater pathogen growth before an immune response begins, while increasing the half-saturation for pathogen growth in the activation function  $f(A)$  (7) has a *negative* effect on blip size, as the slope of the “activation curve” for target cells becomes gentler (Figures 6C,D).

A complex but more biologically realistic version of this model would allow proliferation of the antigen-specific target pool - yielding more activated target cells at the effector stage - and might also allow infection of the proliferating division classes. This would boost the amplitude of the transient and lower the value of  $k_A$  required to produce detectable viremia, thus addressing two flaws in the present model (8). We explore both of these options below.



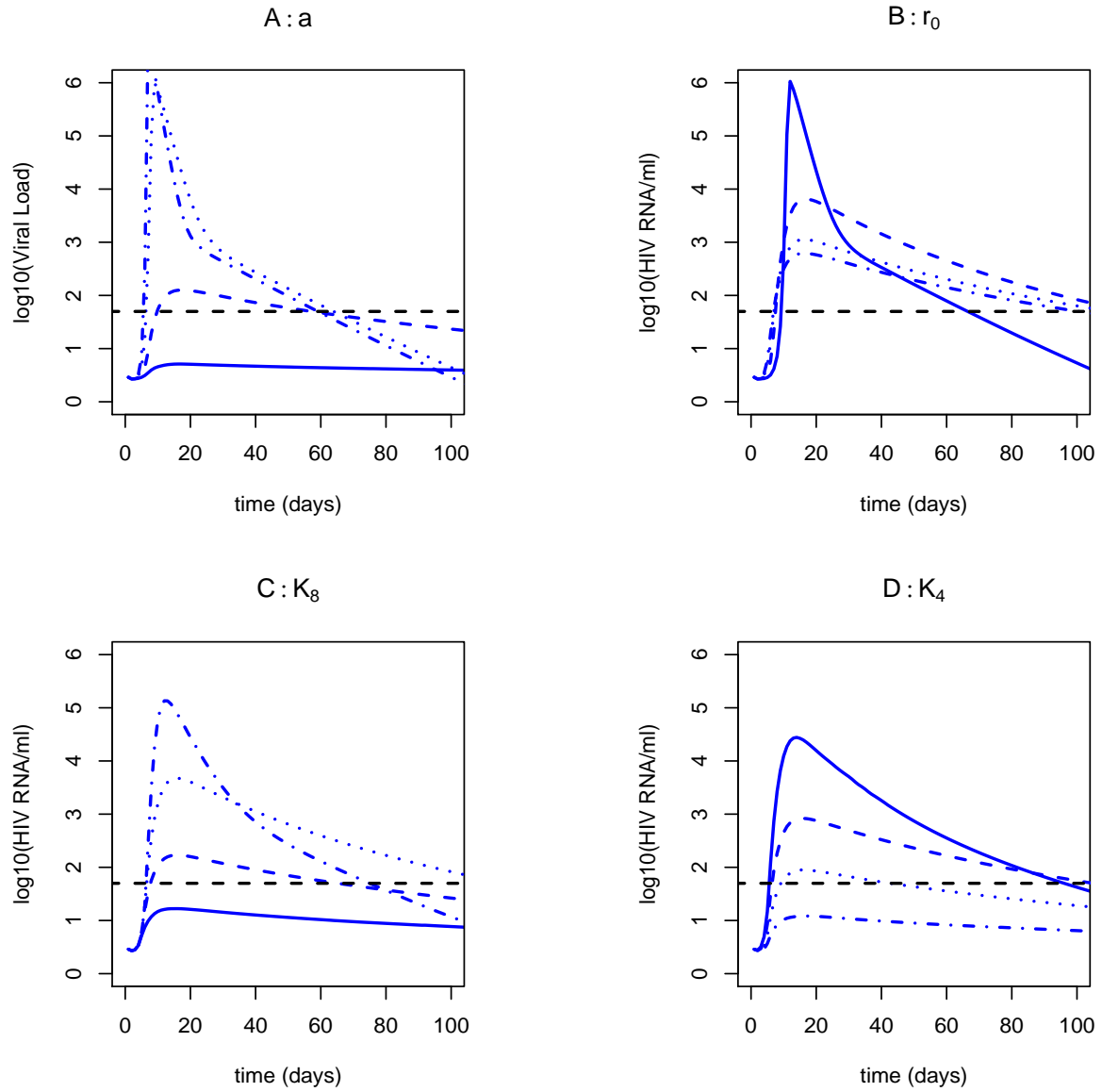


Figure 6: Sensitivity testing, equations (8). Unvaried parameters are as in Figure 5. A, Viral load as the activation parameter  $a$  varies from 0.5 (solid line) to 1.5 (dash-dotted line); B, Viral load as pathogen growth rate  $r_0$  varies from 1 (solid line) to 4 (dash-dotted line); C, Viral load as  $K_8$  (4) varies from  $10^2$  (solid line) to  $10^5$  (dash-dotted line); D, Viral load as  $K_4$  (7) varies from 1 (solid line) to  $10^3$  (dash-dotted line).

## Programmed proliferation of both CD8+ (effector) and antigen-specific CD4+ (target) cells

CD4+ T cells as well as CD8+ T cells undergo programmed proliferation upon exposure to antigen (Lee et al., 2002). These proliferating cells are more susceptible to HIV infection than resting cells. Thus incorporating CD4 cell proliferation cascades should affect HIV replication. We incorporate CD4+ proliferation of antigen-specific CD4+ T cells, with each proliferating division class after the first division assumed activated and thus infectable by HIV-1. The model is identical to equations (8), with the addition of sets of equations for the proliferating  $T_0, T_i, \dots$  classes, and the infected  $T_1^*, T_2^*, \dots$  classes.

As in prior models we assume CD8+ cells undergo eight divisions, so there are eight division classes with the assumption of effector status after the fourth division. CD4+ T cells have slower kinetics than CD8+ T cells, and undergo fewer programmed cycles of proliferation. In the case of LCMV infection of mice this results in 20-fold lower expansion and a delay by one day until the peak of expansion is reached (De Boer et al., 2003). To limit introduction of new parameters, and because little is known about human CD4+ proliferation rates, we assume the same proliferation rates for CD8+ and CD4+ cells. Since CD4+ cells undergo fewer divisions, we assume four CD4+ division classes as opposed to eight, and further assume that they are activated by pathogen and infectable after the first division, and that they suffer elevated mortality  $\delta_A$  when activated. In addition, we allow continued proliferation (division) of infected division classes, which divide to produce infected cells. The initial number of naive cells in both the CD8+ (i.e.,  $N_0$ ) and CD4+ (i.e.,  $T_0$ ) pools is set at 500 cells. To the model for programmed proliferation of CD8 effectors under antigenic stimulation we add the following equations for proliferation and infection of antigen-specific CD4 cells and the passive infection of the nonspecific CD4 pool:

$$\text{Antigen-specific CD4} \quad \frac{dT_0}{dt} = -(p_0(A) + d_0)T_0 \quad (9a)$$

$$\frac{dT_1}{dt} = 2p_0(A)T_0 - (p + d)T_1 - (1 - \epsilon)k_A VT_1 \quad (9b)$$

$$\frac{dT_i}{dt} = \begin{cases} 2pT_{i-1} - (p + d)T_i - (1 - \epsilon)k_A VT_i, & i = 2, 3 \\ 2pT_i - (1 - \epsilon)k_A VT_{i+1} - d_{T_A} T_{i+1}, & i = 4 \end{cases} \quad (9c)$$

$$\frac{dT_1^*}{dt} = (1 - \epsilon)k_A VT_1 - (\delta^*(\omega) + p)T_1^* \quad (9d)$$

$$\frac{dT_i^*}{dt} = \begin{cases} (1 - \epsilon)k_A VT_i + 2pT_{i-1}^* - (\delta^*(\omega) + p)T_i^*, & i = 2, 3 \\ (1 - \epsilon)k_A VT_i + 2pT_{i-1}^* - (\delta^*(\omega))T_i^*, & i = 4 \end{cases} \quad (9e)$$

$$\text{Non-specific CD4} \quad \frac{dT}{dt} = \lambda - (1 - \epsilon)kVT - d_T T \quad (9f)$$

$$\frac{dT^*}{dt} = (1 - \alpha)(1 - \epsilon)kVT - (\delta^*(\omega))T^* \quad (9g)$$

$$\frac{dC}{dt} = \alpha(1 - \epsilon)kVT - \mu^*(\omega)C \quad (9h)$$

$$\frac{dV}{dt} = q_1 T^* + q_2 C + q_3 \sum T_i^* - cV \quad (9i)$$

where  $E = \sum_{i=4}^8 N_i$  and  $p_0(A)$  is defined in equation (4).

Figures 7 and 8 show simulation results and sensitivity testing for equations (9). Figure 7A shows viral load, panel B shows productively and chronically infected cells (solid and dashed line, respectively), and panel C shows infected antigen-specific CD4+ effectors (bold solid line) and division classes (thin dashed line) for a representative parameter set ( $r_0 = 2 \text{ d}^{-1}$ ,  $K_8 = 10^3$ , and  $k_A = 6 \times 10^{-6}$ ). The rise in infected and chronically infected cells from the non-specific pool is fairly small, but most of the new replication in the transient is coming from infection of the even smaller activated antigen-specific pool. The timing of the peak in new productively and chronically infected cells from the non-specific pool is too late to account for the bulk of the viremia in the transient.

The model is fairly robust, producing viral transients of biologically reasonable amplitude and duration over a range of parameter values. In Figure 8 we test the model for reasonable variation in three parameters critical to pathogen growth and viral replication. Results for all three tests are shown in linear scale, as the variation in peak viremia spanned only one order of magnitude. Panel A shows variation in viral load (copies/ml) as  $r_0$  is varied from  $r_0 = 1 \text{ d}^{-1}$  to  $r_0 = 4 \text{ d}^{-1}$ , while parameters  $K_8$  and  $k_A$  are held at the values listed above, and all other parameters are held constant as listed in Table 1. Unlike the prior model (equations 8 and Figures 5 and 6), in this case peak viral load is an increasing function of  $r_0$ , though the increases in VL with each increase in  $r_0$  are moderate. In panel B,  $r_0$  is again set to  $r_0 = 2 \text{ d}^{-1}$ , and the parameter  $K_8$  is varied from  $10^2$  (solid line) to  $10^5$

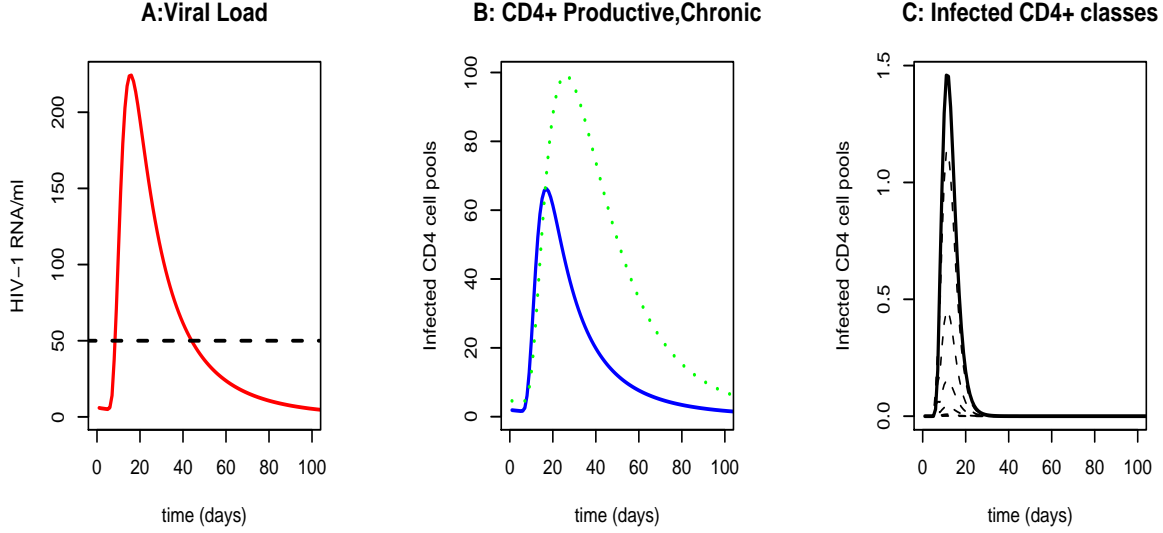


Figure 7: Simulation of equations (9). Again a patient is assumed to be at steady state ( $\bar{V} = 3$  copies/ml) when at  $t = 0$  a growing pathogen is encountered. Here,  $k_A = 4 \times 10^{-6}$  ml/d,  $r_0 = 2.0$  d $^{-1}$  and  $\gamma = 1 \times 10^{-3}$  ml/d. Other parameters are as described in text and shown in Table 1. A, Viral load (copies/ml); dashed line shows limit of assay detection at 50 (copies/ml). B, Total productively (solid line) and chronically infected CD4+ cells (dashed line), C, Infected antigen-specific CD4+ effectors, solid line, plotted with infected antigen specific CD4+ division classes, thin dashed line.

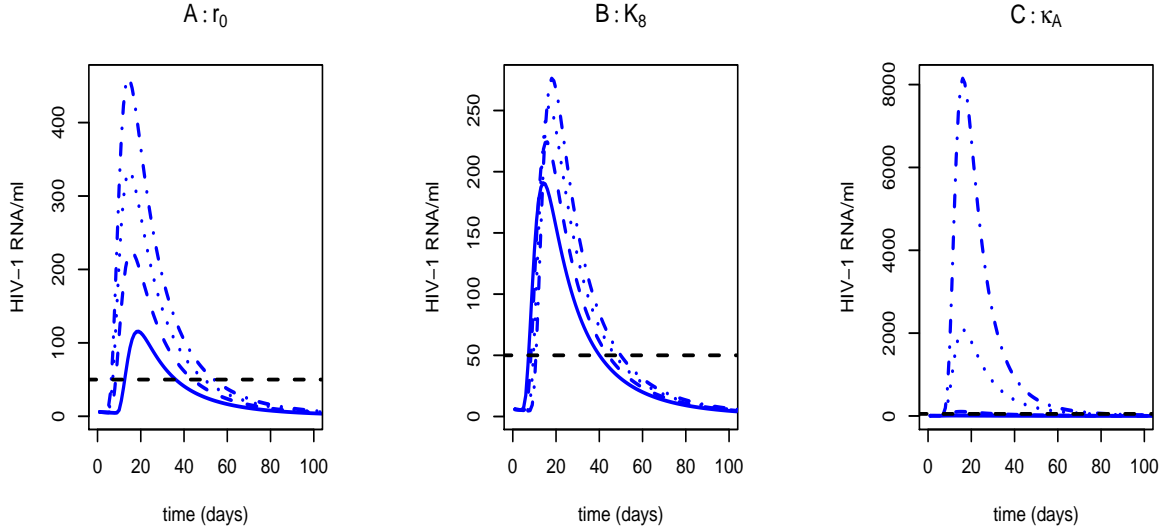


Figure 8: Sensitivity testing for equations (9). Each panel shows viral load (copies/ml) on a linear scale. A, Viral load as pathogen growth parameter varies,  $r_0 = 1, 2, 3, 4$  d $^{-1}$  in solid, dashed, dotted, and dot-dash line, respectively; B, Viral load as  $K_8$  (4) varies from  $10^2$  (solid line) to  $10^5$  (dash-dotted line); C, Viral load due to variation in antigen-specific, activated cell infectivity  $k_A = 8 \times 10^{-7}$  (cf. Callaway and Perelson, 2002),  $1.6 \times 10^{-6}$ ,  $3.2 \times 10^{-6}$ ,  $6.4 \times 10^{-6}$ ,  $8.0 \times 10^{-6}$  (ml $\cdot$ RNA $^{-1}$ d $^{-1}$ ); solid, dashed, dotted, and dot-dash line, respectively.

(dash-dotted line), resulting once again in moderate increases in peak viral load and blip duration. Variations in the infectivity of the antigen-specific cells  $k_A$  over a biologically reasonable range of values also results in moderate and acceptable increases in peak blip viremia (Figure 8C).

## Models with heterogeneous target pools

Another intuitive explanation for the presence of intermittent viremia is to assume that different cell types, or cell populations, might have different drug penetrances, perhaps due to different levels of expression of P-glycoproteins that have the potential to pump drugs out of cells (Kim *et al.*, 1998). Having cell populations with reduced drug penetration may produce episodes of transient viremia in the presence of opportunistic infection. Indeed, there is evidence from *in vitro* studies of heterogeneity in intracellular drug concentrations (*cf.* Kim *et al.*, 1998; Perno *et al.*, 1998; Puddu *et al.*, 1999). In the following model we include two co-circulating populations of target cells with differing drug penetration, wherein drug efficacy is reduced in one cellular population. This is, in addition, a simple means of producing low steady-state viral loads in the presence of drug therapy which does not invoke density dependent mortality of infected cells (*cf.* Callaway and Perelson, 2002).

The model again includes expansion of antigen-specific CD8+ cells, with the effector class  $E$  as the final division class. Effector cells have the same mortality as mature CD4+ T-cell classes, but remain decoupled from the two co-circulating CD4+ classes  $T_1$  and  $T_2$ . Target cells do not proliferate from the naive state but are assumed to have passive sources  $\lambda_1$  and  $\lambda_2$  (Callaway and Perelson, 2002). The model assumes differential drug efficacy in the co-circulating target cell populations: in one population ( $T_1$ ), drug efficacy is  $\epsilon$ , and in the second population ( $T_2$ ), drug efficacy is  $f\epsilon$ , where efficacy has been reduced by a factor  $f < 1$ . Finally, the model includes two separate chronically infected cell pools,  $C^*$ , derived from infected non antigen-specific T-cell pools,  $T_1^*$  and  $T_2^*$ . Again, the model for programmed proliferation of antigen-specific CD8 effector cells is as in (3).

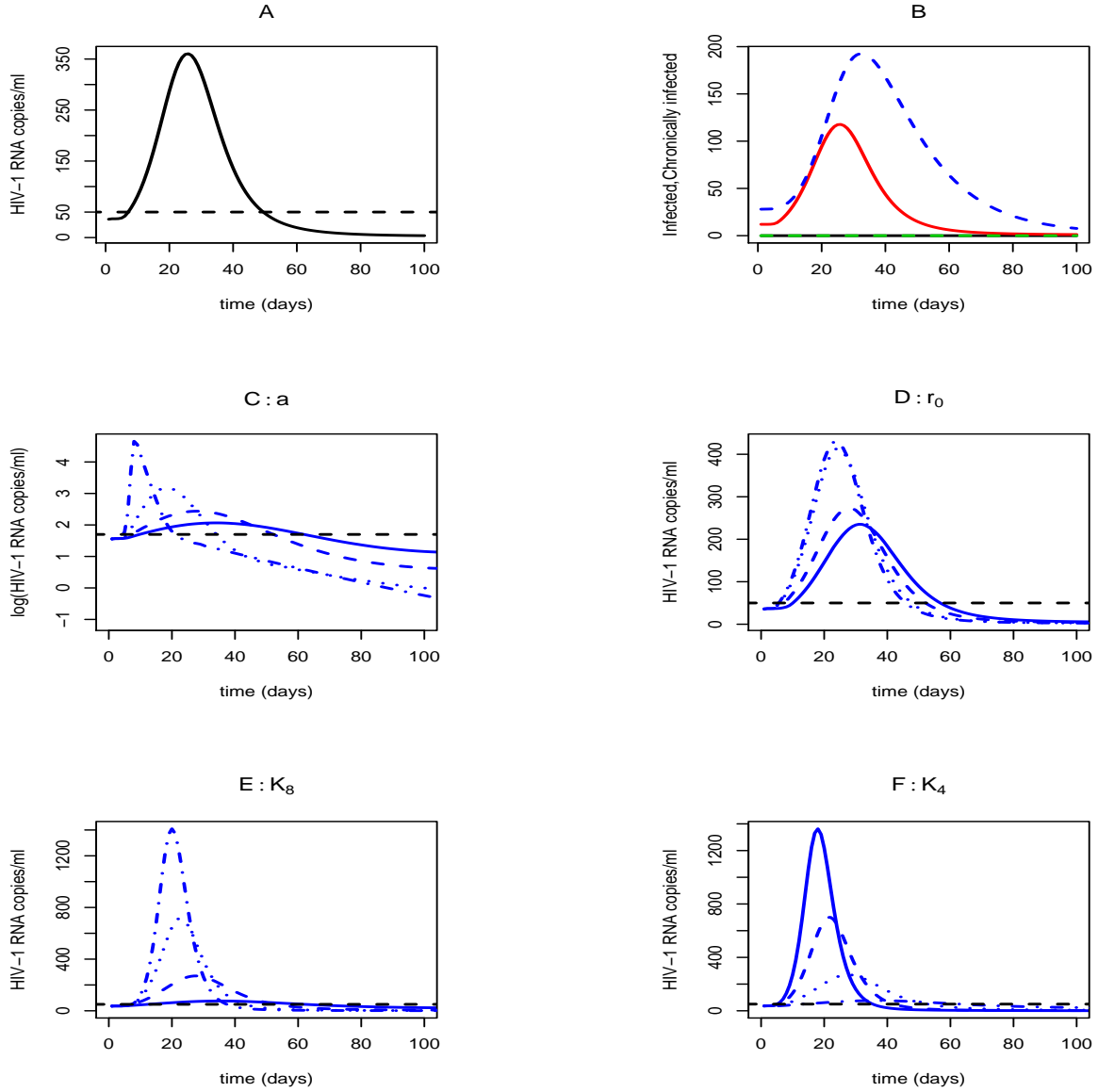


Figure 9: Simulation of equations (10). Here,  $k_1 = 8 \times 10^{-7}$ ,  $k_2 = 1 \times 10^{-5}$  and other parameters are as described in text and shown in Table 1. A, viral load (solid line, in RNA copies/ml) assuming  $r_0 = 2.0$  and  $\gamma = 1 \times 10^{-3}$ . B, Productively and chronically infected CD4+ cells, dashed and solid lines respectively. Note that these cells are contributed only by the cellular pool for which drug efficacy is assumed to be imperfect. C, Viral load ( $\log_{10}$ ) as the activation parameter  $a$  varies from 0.01 (solid line) to 1 (dash-dotted line); D, Viral load (linear scale) as pathogen growth rate  $r_0$  varies from  $1d^{-1}$  (solid line) to 4 (dash-dotted line); E, Viral load as  $K_8$  (4) varies from  $10^2$  (solid line) to  $10^5$  (dash-dotted line); F, Viral load as  $K_4$  (7) varies from  $10^1$  (solid line) to  $10^4$  (dash-dotted line).

$$\frac{dT_1}{dt} = \lambda_1 + f(A)T_1 - (1 - \epsilon)k_A VT - \delta T \quad (10a)$$

$$\frac{dT_2}{dt} = \lambda_2 + f(A)T_2 - (1 - f\epsilon)k_2 VT - \delta T \quad (10b)$$

$$\frac{dT_1^*}{dt} = (1 - \epsilon)(1 - \alpha)kVT_1 - \delta T_1^* \quad (10c)$$

$$\frac{dT_2^*}{dt} = (1 - f\epsilon)(1 - \alpha)kVT_2 - \delta T_2^* \quad (10d)$$

$$\frac{dC_1}{dt} = \alpha(1 - \epsilon)kVT_1 - \mu C_1 \quad (10e)$$

$$\frac{dC_2}{dt} = \alpha(1 - f\epsilon)kVT_2 - \mu C_2 \quad (10f)$$

$$\frac{dV}{dt} = N_T \delta (T_1^* + T_2^*) + N_c \mu (C_1 + C_2) - cV \quad (10g)$$

where again  $E = \sum_{i=4}^8 N_i$ ,  $p_0(A)$  is as in equation (4), and  $f(A)$  is as in equation (7). CD8 effector cells are activated by antigen following a type-II functional response, as in the basic model (6). As in equations (3), CD4+ cells in both pools are activated following a type-II functional response, with activation parameter  $a$ . Other parameters are as defined above and in Table 1, with the exception of parameters specific to a given target cell pool, which are given subscripts appropriate to that pool. Infection rates  $k_A$  and  $k_2$  and cell production rates  $\lambda_1$  and  $\lambda_2$  are thus specific to target cell pools  $T_1$  and  $T_2$ , respectively. As in Callaway and Perelson (2002), we do not introduce different infected cell death rate constants  $\delta$  and  $\mu$  for the differing target cell types. Assuming that  $\epsilon = 1$  in population 1, the steady state viral load is

$$\bar{V}(\epsilon = 1) = \frac{\lambda_2}{c} [(1 - \alpha)N_T + \alpha N_c] - \frac{d_2}{(1 - f)k_2}. \quad (11)$$

Further assuming that  $\bar{V} = 100$  when  $f = 0$ , we set  $\lambda_2 = 57$  cells (ml<sup>-1</sup> d<sup>-1</sup>, see Appendix) and  $k_2 = 10^{-4}$  ml copies<sup>-1</sup> d<sup>-1</sup>, again as in Callaway and Perelson (2002).

In Figure 9 are shown simulations and sensitivity testing of (10). Panel A shows viral dynamics assuming a pathogen with growth rate  $r_0 = 2$ ; viral load is shown in solid line and the threshold for detection [50 copies/ml] is shown dashed. In Figure 9 B is shown the rise in productively and chronically infected cells for both target cell populations. Infected cells for target cell population 1 do not rise at all, so all new viral replication and thus the entire viral transient comes from newly infected cells in population 2. Finally, the above example shows that opportunistic infection will produce viral transients of typical size and duration in numerous models with suitable mechanisms for generating robust low steady-state viral loads.

## Discussion

Models of HIV infection have generally not included detailed models of immune responses. When immune responses are included in such models, they tend to be very stylized, phenomenological rather than mechanistic, and with simple predator-prey type dynamics (cf., Nowak and Bangham, 1996; Wodarz et al., 2000; Wodarz and Nowak, 2000). Recent experimental work has shown that both the CD4+ and CD8+ classes of T cells undergo bursts of proliferation on encounter with antigen, and that programmed proliferative responses continue even if antigen is removed (Badovinac et al., 2002). This is a feature that has not previously been included in HIV models, and one that is especially important to consider when simulating the effects of coinfection - infection with a growing pathogen - on chronically infected HIV patients.

Here we have built a set of models of increasing realism that captures the proliferative response of both CD8+ and CD4+ T cells, and the dynamics of chronic HIV infection in the presence of opportunistic infection. In order to tie our models to data we have focused on explaining the rare occurrences of transient episodes of viremia, or viral blips, that are seen in patients treated with potent antiretroviral therapy. Blip frequency is independent of time on treatment, and if viral loads were to continue to fall towards extinction as they do in most standard models, one would expect the occurrence of detectable viral transients to become rarer with increased time on treatment, something which is not observed (Di Mascio et al., 2003a). Furthermore, chronically infected patients are usually on therapy and their viral loads are generally suppressed below, or close to, the level of detection by standard assay. For these reasons we focused our analysis on HIV models that allow robust low steady state viral loads (Callaway and Perelson, 2002).

### *Simulation results*

Starting from a very simple model of T cell and HIV dynamics under drug therapy (equations 1), which when challenged with a growing pathogen only produced a gradual increase in viral load rather than a blip (Figure 1C) we built a family of new models, at each step adding more biological realism and complexity. The results from each successive interim model guided us towards the creation of biologically realistic and robust end-models, which are capable of producing viral transients of “typical” duration and amplitude, under a biologically reasonable parameter regime.

Addition of a proliferating effector pool and density dependent infected cell death to the initial model results in a model which can produce viral transients, but with an inherent trade-off between blip duration and amplitude (equations 6). The model either produces a blip of appropriate duration, but of amplitude several orders of magnitude larger than desired, or of appropriate amplitude, and upwards of 100 days duration (Figure 4) depending on the choice of parameters. This appears to be due to the fact that in the model the entire



pool of CD4+ cells is activated by antigen, resulting in a large spike in viral replication. In addition, this large target pool has the low mortality assumed for “resting” cells, which affects the duration of the resulting blips.

We then separate the target pool into antigen specific and non-specific CD4+ T cells, and allow activation by antigen - and thus increased susceptibility to infection - of the antigen-specific pool (equations 8). Simulations of this model can produce blips with a sharp rise-time and slow decay, consistent with observation, and of “typical” amplitude as described above. However, even the smaller ( $< 100$  RNA copies/ml) blips are slightly too long in duration (30 days) (Figure 5A), and the model is very sensitive to changes in the activation parameter  $a$  and the half-saturation constant  $K_8$ , both of which are difficult to quantify via experiment or observation.

Allowing the antigen-specific target cell pool to proliferate upon exposure to antigen is a natural next step, which eliminates the biologically ambiguous activation parameter,  $a$ , and produces a model which generates “blips” of reasonable amplitude and duration over a range of parameter values (equations 9; Figure 8)

A model that includes cell populations with different drug susceptibilities (equations 10) generates robust low steady state viral loads without having to invoke density-dependent cell death and its attendant parameters (cf. Callaway and Perelson, 2002). This model when coupled with a CD8+ T cell model of the response to a replicating antigen, can also produce viral transients of appropriate amplitude and duration. In this case it is interesting to note that the viral transient arises entirely from the second compartment with reduced drug penetration; thus the size and duration of such transients might scale with the size of the compartment from which they arise.

### *Limitations*

The models presented here, despite their increasing complexity, remain simplifications of an in vivo system. In order to limit the size of our models and the number of parameters therein, we have not included HIV-specific CD8+ and CD4+ T cells. In addition, we have focused entirely on a T-cell mediated immunity, and have not included antibody (B-cell) responses.

The clonal expansion and survival of CD8+ T cells may depend on the activity and “help” of CD4+ T cells, but mostly during formation of memory and during antigen rechallenge (Bevan, 2004). Thus *primary* CD8+ T cell responses are undiminished in a CD4+ T cell deficient system: when antigen alone invokes an overwhelming inflammatory response, as in many infections, primary CD8+ T cell responses are entirely independent of the CD4+ T cell response (Bevan, 2004). Yet CD8+ T cell memory during antigen *rechallenge* does not function properly in a CD4+ T cell deficient system. Furthermore, there is some evidence that frequency of viral transients is statistically correlated with low CD4+ counts (Di Mascio et al., 2003a). It would be worth exploring whether, in a CD4+ T cell deficient environment,

insufficient CD8+ T cell responses to chronic immune rechallenge contribute to episodes of transient viremia. While we do not include CD4+ “help”, or indeed, CD8+ T cell memory in our system, these features would be necessary for any biologically realistic simulation of an immune system encountering pathogens in a stochastic fashion. We have omitted these features here as we have not modeled antigen rechallenge and immune memory. Our future research interests include stochastic exploration of immune activation during random encounters (and re-encounters) with pathogen, and thus will invoke immune memory.

### *Conclusions*

We have shown that episodes of transient viremia in otherwise well-suppressed, chronically infected HIV patients under drug therapy may be triggered by randomly-occurring opportunistic infections, which cause a rise in activated target cells, and thus transient bursts of infection and resultant viremia. Simple models for coinfection, which incorporate stylized, predator-prey type immune dynamics, cannot account for the occurrence of viral transients. However, if biologically realistic T cell dynamics that include programmed proliferation and contraction of the CD8+ T cell are incorporated into the model, along with a mechanism for producing robust low steady-state viral loads under HAART, then we have shown that opportunistic infection can serve as a “forcing function” for transient episodes of viral replication and can explain the observation of viral blips in otherwise well-suppressed HIV patients. This is just one plausible mechanism among many for the generation of blips; the list of possible causes also includes missed drug doses, activation of latently infected cells and release of virus from tissue reservoirs. It remains to be shown that these other mechanisms also work in a model and produce transients of appropriate amplitude and duration.

## **Acknowledgements**

This research was supported by the Department of Energy under contract W-7405-ENG-36 and by NIH grants AI28433 and RR06555 (ASP). We thank Michele Di Mascio for the data used in Figure 1. We thank Rob DeBoer for many useful discussions on the topic of T-cell proliferation, and the Cornell EEB eco-theory lunch-bunch, in particular Stephen Ellner, for comments which greatly improved this paper.

## Appendix

All simulations were written in the **R** programming language (version 1.9) and run on a Windows XP platform, using the **odesolve** package.

Steady state values were obtained numerically by setting fixed parameter values and running the model until the simulation reached steady state. Steady state values for each variable were noted and used as initial conditions for simulations of the effect of concurrent infection.

### Parameter values:

$\epsilon$ : for the chronically infected cell model (1), we seek a steady state viral load  $\bar{V}$  of around 50 copies/ml. Solving the expression for steady state viral load (2) for  $\epsilon$ , we obtain:

$$\epsilon = 1 - \frac{dc/\kappa}{\lambda[(1-\alpha)N_T + \alpha N_C] - c\bar{V}}.$$

Substituting in the appropriate parameters, one obtains a required drug efficacy of about 0.6458 for a steady state viral load of  $\bar{V} \doteq 50$ . This efficacy is close to the critical efficacy for the models presented here, given our parameters.

$\lambda_2$ : In the two-compartment co-circulating cell model (10), we invoke the expression for steady-state viral load, assuming  $\epsilon = 1$  in the first cellular pool (11). Solving for the parameter  $\lambda_2$ :

$$\lambda_2 = c \frac{\bar{V} \kappa_2 (1 - f) + d_2}{\kappa_2 (1 - f) [(1 - \alpha) N_T + \alpha N_C]}$$

Further assuming that  $\bar{V} = 100$  when  $f = 0$  and substituting in appropriate parameter values gives a value  $\lambda_2 \doteq 57$ .

$\mu'$ : Observing that the ratio  $\delta : \mu = 10$  for the death rates of productively versus chronically infected cells (Callaway and Perelson, 2002) we retain the same ratio of death rates under the assumption of density dependent mortality for both cellular pools. Thus, if  $\delta' = 0.7863 d^{-1} (ml \cdot cell^{-1})^\omega$ , then  $\mu' = 0.07863 d^{-1} (ml \cdot cell^{-1})^\omega$ .

## References

- [1] Badovinac, V. P., B. B. Porter and J.T. Harty (2002). Programmed contraction of CD8+ T cells after infection. *Nature Immunol.* **3**, 619-626.
- [2] Bevan, M. J. (2004). Helping the CD8+ T-cell response. *Nature Rev. Immunol.* **4**, 595-602.
- [3] Brichacek B., S. Swindells, E. N. Janoff, S. Pirruccello, and M. Stevenson (1996). Increased plasma human immunodeficiency virus type 1 burden following antigenic challenge with pneumococcal vaccine. *J. Infect. Dis.* **174**, 1191-1199.
- [4] Callaway, D. S. and A. S. Perelson (2002). HIV-1 infection and low steady state viral loads. *Bull. Math. Biol.*, **64**, 29-64.
- [5] De Boer, R. J., M. Oprea, R. Antia, K. Murali-Krishna, R. Ahmed, and A. S. Perelson (2001). Recruitment times, proliferation, and apoptosis rates during the CD8+ T cell response to LCMV. *J. Virol.* **75**, 10663-10669.
- [6] De Boer, R. J., D. Homann and A. S. Perelson (2003). Different dynamics of CD4+ and CD8+ T cell responses during and after acute lymphocytic choriomeningitis virus infection. *J. Immunol.* **171**, 3928-3935.
- [7] De Boer, R. J. and A. S. Perelson. Estimating division and death rates from CFSE data. *J. Comput. Appl. Math.* (in press).
- [8] Deenick, E. K., A. V. Gett and P. D. Hodgkin (2003). Stochastic model of T cell proliferation: A calculus revealing IL-2 regulation of precursor frequencies, cell cycle time, and survival. *J. Immunol.* **170**, 4963-4972.
- [9] Di Mascio, M., M. Markowitz, M. Louie, C. Hogan, A. Hurley, D. D. Ho, and A. S. Perelson (2003a). Viral blip dynamics during highly active antiretroviral therapy. *J. Virol.* **77**, 12165-12172.
- [10] Di Mascio, M., G. Dornadula, H. Zhang, J. Sullivan, Y. Xu, J. Kulkosky, R. Pomerantz and A. S. Perelson (2003b). In a subset of patients on highly active antiretroviral therapy plasma HIV-1 RNA can decay from 50 copies/ml to < 5 copies/ml with a half-life of six months. *J. Virol.* **77**, 2271-2275.
- [11] Di Mascio, M., R. M. Ribiero, M. Markowitz, D. D. Ho, and A. S. Perelson (2004a). Modeling the long-term control of viremia in HIV-1 infected patients treated with antiretroviral therapy. *Math. Biosciences* **188**, 47-62.
- [12] Di Mascio, M., M. Markowitz, M. Louie, A. Hurley, C. Hogan, V. Simon, D., Follman, D. D. Ho, and A. S. Perelson (2004b). Dynamics of intermittent viremia during highly

- active antiretroviral therapy in patients who initiate therapy during chronic versus acute and early human immunodeficiency virus type 1 infection. *J. Virol.* **78**, 10566-10573.
- [13] Dornadula, G., Zhang, H., VanUitert, B., Stern, J., Livornese, L. Jr., Ingerman, M. J., Witek, J., Kedanis, R. J., Natkin, J., DeSimone, J., and Pomerantz, R. J. (1999). Residual HIV-1 RNA in blood plasma of patients taking suppressive highly active antiretroviral therapy. *J. Amer. Med. Assoc.* **282**, 1627-1632.
- [14] Ferguson N. M., F. deWolf, A. C. Ghani, C. Fraser, C. A. Donnelly, P. Reiss, J. M. A. Lange, S. A. Danner, G. P. Garnett, J. Goudsmit, and R. M. Anderson (1999). Antigen-driven CD4+ T-cell and HIV-1 dynamics: residual viral replication under highly active antiretroviral therapy. *Proc. Natl. Acad. Sci. USA* **96**, 15167-15172.
- [15] Gett, A. V. and P. D. Hodgkin (2000). A cellular calculus for signal integration by T cells. *Nature Immunol.* **1**, 239-244.
- [16] Holte, S. A., A. Melvin, J. Mullins, and L. Frenkel (2001). Density-dependent decay in HIV dynamics after HAART (Abstract 394), in *8th Conference on Retroviruses and Opportunistic Infections*, Alexandria, VA, USA: Foundation for Retrovirology and Human Health.
- [17] Jones, L. E. and A. S. Perelson (2002). Modeling the effects of vaccination on chronically infected HIV-positive patients. *JAIDS* **31**, 369-377.
- [18] Kaech, S. M. and R. Ahmed (2001). Memory CD8+ T cell differentiation: initial antigen encounter triggers a developmental program in naive cells. *Nature Immunol.* **2**, 415-422.
- [19] Kim R.B., M. F. Fromm, C. Wandel, B. Leake, A. J. Wood, D. M. Roden, and G. R. Wilkinson (1998). The drug transporter P-glycoprotein limits oral absorption and brain entry of HIV-1 protease inhibitors. *J. Clin. Invest.* **101**, 289-294.
- [20] Lee, W. T., Pasos, G., Cecchini, L. and Mittler, J. N. (2002). Continued antigen stimulation is not required during CD4+ T cell clonal expansion. *J. Immunol.* **168**, 1682-1689.
- [21] McLean, A. R., and M. A. Nowak (1992). Models of interactions between HIV and other pathogens. *J. Theor. Biol.* **155**, 69-102.
- [22] Mittler, J. E., M. Markowitz, D. D. Ho and A. S. Perelson (1999). Improved estimates for HIV-1 clearance rate and intracellular delay. *AIDS* **13**, 1415-1417.
- [23] Mohri, H., S. Bonhoeffer, S. Monard, A. S. Perelson and D. D. Ho (1998). Rapid turnover of T-lymphocytes in SIV-infected rhesus macaques. *Science* **279**, 1223-1227.

- [24] Murali-Krishna, K., J. D. Altman, M. Suresh, D. Sourdive, A. Zajac, J. D. Miller, J. Slansky and R. Ahmed (1998a). Counting antigen-specific CD8 T cells: a reevaluation of the bystander activation during viral infection. *Immunity* **8**, 177-187.
- [25] Murali-Krishna, K., J. D. Altman, M. Suresh, D. Sourdive, A. Zajac, and R. Ahmed (1998b). *In vivo* dynamics of antiviral CD8+ T cell responses to different epitopes: an evaluation of bystander activation in primary and secondary responses to viral infection. *Adv. Exp. Med. Biol.* **452**, 123-142.
- [26] Nowak, M. A. and C. R. M. Bangham (1996). Population dynamics of immune responses to persistent viruses. *Science* **272**, 74-79.
- [27] Nowak, M. A. and May, R. M. (2000). *Virus dynamics: Mathematical Principles of Immunology and Virology*. Oxford University Press, Oxford.
- [28] O'Brien W. A., K. Grovit-Ferbas, A. Namazi, S. Ovcak-Derzic, H. J. Wang, J. Park, C. Yeramian, S. H. Mao, and J. A. Zack (1995) Human immunodeficiency virus type 1 replication can be increased in the peripheral blood of seropositive patients after influenza vaccination. *Blood* **86**, 1982-1089.
- [29] Perelson, A. S., A. U. Neumann, M. Markowitz, J. M. Leonard, and D. D. Ho (1996). HIV-1 dynamics in vivo: Virion clearance rate, infected cell lifespan, and viral generation time. *Science* **271**, 1582-1586.
- [30] Perelson A. S., P. Essunger, Y. Cao, M. Vesanen, A. Hurley, K. Saksela, M. Markowitz and D. D. Ho (1997). Decay characteristics of HIV-1 infected compartments during combination therapy. *Nature* **271**, 1582-1586.
- [31] Perelson, A. S. (2002). Modelling viral and immune system dynamics. *Nature Rev. Immunol.* **2**, 28-36.
- [32] Perno C., F. M. Newcombe, D. Davis, S. Aquaro, R. W. Humphrey, R. Calio and R. Yarchoan (1998). Relative potency of protease inhibitors in monocytes/macrophages acutely and chronically infected with human immunodeficiency virus. *J. Infect. Dis.* **178**, 413-422.
- [33] Puddu, P., S. Fais, F. Luciani, G. Gherardi, M. L. Dupuis, G. Romagnoli, C. Ramoni, M. Cianfriglia and S. Gessani (1999). Interferon- $\gamma$  up-regulates expression and activity of P-glycoprotein in human peripheral blood monocyte-derived macrophages. *Lab. Invest.* **79**, 1299-1309.
- [34] Revy, P., M. Sospedra, B. Barbour, and A. Trautman (2001). Functional antigen-independent synapses formed between T-cells and dendritic cells. *Nat. Immunol.* **2**, 925-931.

- [35] Sachsenberg N., A. S. Perelson, S. Yerly, G. A. Schockmel, D. Leduc, B. Hirschel, and L. Perrin (1998). Turnover of CD4+ and CD8+ T Lymphocytes in HIV-1 Infection as Measured by Ki-67 Antigen. *J. Exp. Med.* **187** (8) 1295-1303.
- [36] Stanley S. K., M. A. Ostrowski, J. S. Justement, K. Gantt, S. Hedayati, M. Mannix, K. Roche, D. Schwartzentruber, C. H. Fox, and A. S. Fauci (1996). Effect of immunization with a common recall antigen on viral expression in patients infected with human immunodeficiency virus type 1. *N. Engl. J. Med.* **334**, 1222-1230.
- [37] Staprans, S. I., B. Hamilton, S. Follansbee, T. Elbeik, P. Barbosa, R. Grant and M. Feinberg (1995). Activation of virus replication after vaccination of HIV-1 infected individuals. *J. Exp. Med.* **182**, 1727-1737.
- [38] Van Stipdonk, M. J., E. E. Lemmons and S. P. Schoenberger (2001). Naive CTLs require a single brief period of antigenic stimulation for clonal expansion and differentiation. *Nature Immunol.* **21**, 29-70.
- [39] Wodarz, D. and M. A. Nowak (2000). CD8 escape, immunodominance, and antigenic escape. *Eur. J. Immunol.* **30**, 2704-2712
- [40] Wodarz, D., R. M. May, and M. A. Nowak (2000). The role of antigen-independent persistence of memory cytotoxic T lymphocytes. *Intl. Immunol.* **12**, 467-477.
- [41] Wong, P. and E. G. Pamer (2003). CD8 T-cell responses to infectious pathogens. *Ann. Rev. Immunol.* **21**, 29-70.
- [42] Zhang, Z. Q., S. W. Wietgreffe, Q. Li, M. D. Shore, L. Duan, C. Reilly, J. D. Lifson, and A. T. Haase (2004). Roles of substrate activity and infection of resting and activated CD4+ T cells in transmission and acute simian immunodeficiency virus infection. *Proc. Natl. Acad. Sci. USA* **101**, 5640-5645.

**Table 1. Model Parameters**

Parameter	Description	Value	Reference
$a$	T-cell activation parameter	variable	
$\alpha$	fraction chronically infected	0.195	CP02
$A_{max}$	pathogen carrying capacity	$10^8$ (units/ml)	
$c$	clearance rate	$23 (d^{-1})$	R99
$d_0$	death rate, quiescent cells	$0.01 (d^{-1})$	DB01
$d$	death rate, division classes	$0.1 (d^{-1})$	Set
$d_{T_A}$	death rate, antigen specific	$0.325 (d^{-1})$	DB03
$d_T$	death rate, non-specific	$0.01 (d^{-1})$	DB01
$\delta$	death rate, infected cells	$0.7 (d^{-1})$	P97
$\delta'$	density dependent mortality	$0.7863$ $d^{-1}(ml \cdot cell^{-1})^\omega$	CP02
$d_E$	death rate, effector cells	$0.325 (d^{-1})$	DB03
$\epsilon$	drug efficacy	$0 < \epsilon < 1$	Appendix
$\gamma$	pathogen clearance rate	$10^{-3} (d^{-1})$	see text
$k, k_1$	infectivity, single(first) target pool	$8 \times 10^{-7}$ $(ml \cdot RNA^{-1} d^{-1})$	CP02
$k_A$	infectivity, Ag-specific target pool	$6 \times 10^{-6}$	set
$k_2$	infectivity, second target pool	$10^{-4}$	CP02
$K, K_8$	antigen half-saturation for stimulating CD8 cells	variable	
$K_4$	antigen half-saturation for stimulating CD4 cells	variable	
$\lambda, \lambda_1$	passive T cell source	$10^4$ (cells /ml/d)	CP02
$\lambda_2$	passive T-cell source	$56$ (cells/ml/d)	Appendix
$\mu_C$	mortality, chronically infected	0.07	P97
$\mu'$	density-dependent mortality	0.07863	Appendix
$N_0, T_0$	initial quiescent population	500 cells	see text
$N_c$	burst size, chronically infected	4.11 RNA copies	CP02
$N_T$	burst size, productively infected	100 RNA copies	CP02
$\nu$	antigen-specific fraction	0.1	S98
$p_0$	initial proliferation rate	$1 (d^{-1})$	DB01
$p$	proliferation rate, classes 1, ..., $k$	$2.92 (d^{-1})$	DB01
$\omega$	See equation (5)	0.01	CP02
$q_1, q_2, q_3$	HIV production, density dependent	$70, 0.28 (d^{-1})$	CP02
$q_3$	HIV production, density dependent	$840 (d^{-1})$	Z04

**CP02:** Callaway and Perelson 2002, **DB01:** De Boer *et al.* 2001, **DB03:** De Boer *et al.* 2003, **P97:** Perelson *et al.* 1997, **S98:** Sachsenberg *et al.* 1998, **Z04:** Zhang *et al.* 2004.